

Thermal Double Donors and Quantum Dots

J. Coutinho and R. Jones

School of Physics, University of Exeter, Exeter EX4 4QL, United Kingdom

L. I. Murin

Institute of Solid State and Semiconductor Physics, Minsk 220072, Belarus

V. P. Markevich

Centre for Electronic Materials, UMIST, Sackville Street, Manchester M601QD, United Kingdom

J. L. Lindström

Department of Physics, University of Lund, S-221 00 Lund, Sweden

S. Öberg

Department of Mathematics, Luleå University of Technology, Luleå S-97187, Sweden

P. R. Briddon

Department of Physics, University of Newcastle upon Tyne, Newcastle upon Tyne NE1 7RU, United Kingdom

(Received 14 August 2001; published 14 November 2001)

Combined local mode spectroscopy and *ab initio* modeling are used to demonstrate for the first time that oxygen atoms in thermal double donors (TDD) in Si are in close proximity. The observed vibrational modes in ^{16}O , ^{18}O , and mixed isotopic samples are consistent with a model involving [110] aligned oxygen chains made up of an insulating core lying between electrically active ends. The model also explains the minute spin density observed on oxygen in TDD^+ as well as the piezospectroscopic tensors of the donors. The analogy between the thermal donors and quantum dots is emphasized.

DOI: 10.1103/PhysRevLett.87.235501

PACS numbers: 61.72.Bb, 63.20.Pw, 81.05.Cy, 81.40.Tv

Thermal double donors (TDD) are formed by heating oxygen-rich Si at temperatures between 350 °C and 500 °C [1]. They comprise a family of at least 17 double donors which form sequentially and are distinguished by their increasingly shallow levels [2]. In spite of extensive studies, they remain a mystery. There are in essence two models to the origin of the donors. The first, much favored in theoretical studies [3], believes that they consist of an increasing number of O atoms, arranged in a [011] chain, surrounding a core containing at least one overcoordinated oxygen defect. The second model, places a silicon interstitial (I_{Si}) or interstitial cluster at the core surrounded by a few oxygen atoms [4,5]. It must be admitted that the bulk of experimental evidence favors the latter.

Three examples reveal the difficulties of the oxygen-only model [2]. First, the activation energy for the transformation of $\text{TDD}(N)$ into $\text{TDD}(N + 1)$ varies from 1.2 eV for $N = 1$, to 1.7 eV for larger N . This rules out a model where single oxygen atoms (O_i) diffuse to an oxygen cluster with an activation energy of 2.5 eV, as well as one involving only mobile dimers as their concentration would be rapidly exhausted [6–8]. Second, magnetic resonance studies on the NL8 signal, assigned to $\text{TDD}(N)^+$, show that the spin density on oxygen atoms is infinitesimally small [9]. The ^{17}O isotropic hyperfine interaction, ~ 0.5 MHz in NL8, is much less than the 3 MHz found in VO^- , in spite of the fact that oxygen in VO^- is located

in a nodal plane of the spin density [10]. How, one wonders, can the source for the donor activity be oxygen when there is so little spin density associated with it? Third, the oxygen-only model requires an increasing number of oxygen-related local vibrational modes (LVMS) to be associated with the later donors, but only at most two such modes have been assigned to any donor [11].

Despite these difficulties with the oxygen-only model, it has not been possible, in spite of many attempts, to produce convincing models of $I_{\text{Si}}\text{O}$ clusters with the properties of the donors: we found, for example, the well-known $I_{\text{Si}}\text{O}_2$ model from Ref. [5] to be unstable. Thus, any credible oxygen-only proposal must also address the three fundamental questions listed previously.

We show here that this model, perhaps surprisingly, can account for the above difficulties. Further, it also *quantitatively* explains the variation of the piezospectroscopic stress-energy tensor, and the LVMS along with their isotopic shifts which are reported for the first time.

The calculations were carried out with the density functional AIMPRO supercell code employing up to 160 Si atoms [12]. The details of the method, including convergence issues, have been given previously in an extensive treatment of oxygen defects in Si and Ge [13].

The first problem to address is oxygen diffusion. We found, in agreement with Ref. [14], that small O chains aligned along [110] can migrate through the lattice with

barriers ~ 1 eV below that of O_i . With isolated oxygen concentrations of 10^{18} cm^{-3} and maximum donor concentrations of 10^{16} cm^{-3} , the diffusing chain will most likely encounter a single oxygen interstitial, either lying in the same or nearby $[110]$ valley. In the latter case, there will have to be single oxygen jumps before a longer chain is formed. It is this rapid chain diffusion which enables long chains to grow rapidly and hence we seek donor activity arising from long chains.

We examined the most stable configuration of nine *periodic infinite* chains along $[110]$. The lowest energy chain is the O_∞ -2NN model shown in Fig. 1(a), where oxygen is bonded to second-neighbor Si atoms in two parallel chains. Both Si and O have their normal coordination. A plot of the charge density revealed ionic bonding across and along the chains. While short O_5 -1NN and O_6 -1NN chains, where oxygen bridges first-neighbor Si atoms, are more stable than O_n -2NN chains by 0.6 and 0.2 eV, respectively, the reverse is true for long ones, with O_7 -2NN lower in energy by 0.1 eV. Hence a crossover occurs at about 6–8 oxygen atoms.

It is tempting to identify the O-2NN chains with the donors. Although they have the same C_{2v} symmetry, this cannot be correct. We found the chain to be insulating with the six $\langle 100 \rangle$ conduction band minima split by the compressive stress due to the oxygen chains. As a result a pair of valleys along $[001]$ is pushed into the gap. The wave function for this empty *stress-induced state*, Fig. 2(a), avoids O atoms and is mainly localized on Si atoms lying within the nearest $(1\bar{1}0)$ planes, consistent with its stress origin and with the nature of the conduction band in ionic materials.

Whereas the infinite chain is insulating, the finite chain is not. A fully occupied state now edges the conduction band [12]. This state must have originated from the end regions but the wave function of this shallow double donor level [shown in Fig. 2(b) for O_9 -2NN], is the *same* stress-induced, but empty, gap state found for the infinite O_∞ -2NN chain.

We understand this as follows. The end O atoms in O_9 -2NN [Fig. 1(b)] are bonded to nearest Si neighbors (O-1NN defects) and the transition from these to the

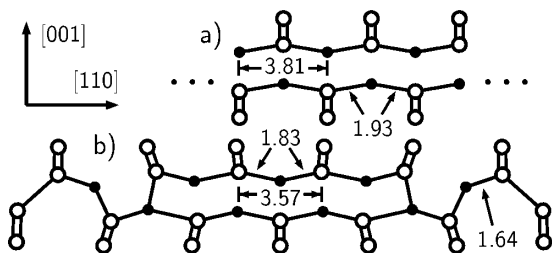


FIG. 1. Most stable structures for (a) *infinite chain* (referred to as O_∞ -2NN) and (b) the TDD model O_9 -2NN finite chain. All lengths are in Å. O and Si are shown as black and white circles, respectively.

O-2NN core must involve a topological defect consisting of either overcoordinated oxygen species [see Fig. 1(b)] or divalent oxygen together with a Si dangling bond. Hydrogenation of the Si dangling bonds at both ends results in normal Si and O coordination and the elimination of the donor behavior consistent with H-passivation studies [15]. This is a direct link between the donor activity and the topological defects. However, Fig. 2(b) can be explained only if the energy levels of the topological defects lie *above* the stress-induced gap level and the donor electrons drop into the latter. Thus the wave function loses its oxygen parentage and this explains the almost infinitesimal spin density found on oxygen in NL8. A simple analogy can be made with an externally doped GaAs quantum dot embedded in AlAs. An electron arising from a Si donor in the AlAs matrix drops into the lower lying unoccupied dot state arising from the band offset between GaAs and AlAs. A magnetic resonance experiment then reveals a spin density on Ga but not on Si. It might be then erroneously concluded that the source of the donor activity is a Ga interstitial. The important point is that these experiments do not reveal the primary cause of donor activity in the thermal donors.

A Mulliken bond population on O_9 -2NN showed about 0.75% for the unique central core Si atom to 0.65% for the end Si atoms. These are in line with ENDOR data giving about 0.3% for several shells of Si atoms, including the unique atom, when it is remembered that the finite supercell leads to an upper bound. The population on oxygen was small, consistent with a very low spin density, but it was negative, making a direct interpretation impossible.

We can now identify the donors with different oxygen chains. The vibrational modes of O_2 and O_3 have been identified and these species are not thermal donors [7]. TDD(0) may be identified with a chain of perhaps four or five O atoms, suggesting that TDD(N) is O_n -2NN with $n = N + 4$ or $N + 5$. This agrees with observations

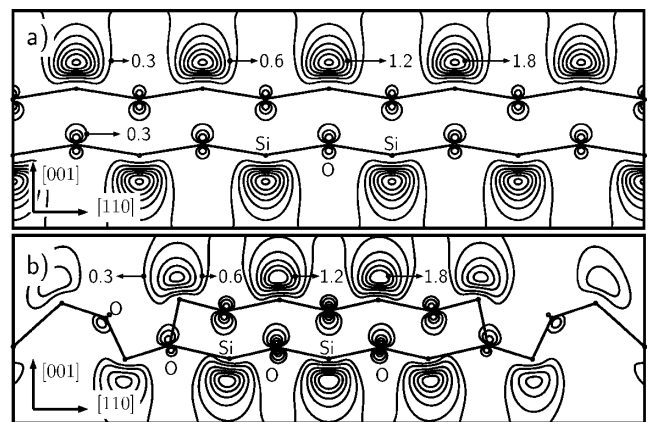


FIG. 2. Squared wave function $(|\psi_{n,\mathbf{k}}(\mathbf{r})|^2 \times 1000)$ for (a) the lowest unoccupied state of O_∞ -2NN and (b) for the highest occupied state in O_9 -2NN. Both states have \mathbf{k} vectors along (001) .

where a loss of about 9–10 oxygen atoms from solution per TDD accompanies the formation of the average donor, taken to be TDD(5) or TDD(6) [4,16]. The bistability of TDD(N) for $N \leq 2$ is also consistent with the calculated metastability of neutral O_n -2NN, with respect to O_n -1NN, for less than 6–8 O atoms.

The compressive stresses exerted by the O-2NN core and O-1NN ends are different. The former lies along [001] and the latter along [111] and $[\bar{1}\bar{1}1]$. Table I shows that the [001] displacement of the central Si atoms decreases with the length of the chain. This reflects an increasing ionic bonding between the chains and implies (i) that the strain-induced level becomes shallower, consistent with the observed shift in the donor level with N , and (ii) the stress energy or piezospectroscopic tensor decreases with N . We have evaluated these tensors in a way described earlier [13]. Table I shows that the calculated tensors for the smaller C_{2v} chains possess principal values very close to, and display the correct trend with, the experimental values. Note that, although O_6 has C_{2h} symmetry, the two principal directions of the tensor are rotated by only $\theta = 9^\circ$ from the [001] and [110] crystallographic axes and it is likely that $\theta \sim 0$ for stress tensors for longer chains with even n .

Further support for the model comes from the observations and analysis of the LVMS associated with each donor. Three types of Si samples were investigated experimentally. The first (spectrum 1) (see Fig. 3) contained ^{16}O , while the second (spectrum 2) contained mainly ^{18}O . The third (spectrum 3) was codoped with ^{16}O and ^{18}O . Thermal donors were generated after heat treatments at 420 °C in air. The IR absorption measurements were carried out at 10 and 300 K using a Bruker 113v Fourier transform IR spectrometer. The spectral resolution was 0.5 or 1.0 cm^{-1} .

Figure 3 (bottom) shows fragments of differential absorption spectra (300 K) of heat treated Si:O samples. A signal recorded from a high-purity float-zone Si sample was subtracted from each spectrum. In sample 1, bands due to TDD(2), TDD(3), and oxygen dimers are dominant

TABLE I. Calculated [001] displacements (\AA), $\delta_c(001)$, $\delta_e(001)$, of central and end Si atoms, and stress-energy tensor elements B along [001] and [110] (eV), for O_n -2NN chains. Observed tensors for the early TDD members were measured by Fourier-transform infrared spectroscopy and EPR (*) [18].

| Calc. | O_5 -2NN C_{2v} | O_6 -2NN C_{2h} | O_7 -2NN C_{2v} | O_∞ -2NN |
|-----------------|---------------------|---------------------|---------------------|-----------------|
| $\delta_c(001)$ | 0.43 | 0.42 | 0.41 | 0.34 |
| $\delta_e(001)$ | 0.22 | 0.22 | 0.22 | – |
| B_{001} | –13.8 | –13.2 | –12.1 | – |
| B_{110} | 10.5 | 9.9 | 8.3 | – |
| Obs. | TDD(2) | TDD(3) | TDD(4) | |
| B_{001} | –12.2 | –11.9 | –11.4 | |
| B_{110} | | 10.3* | 8.5* | |

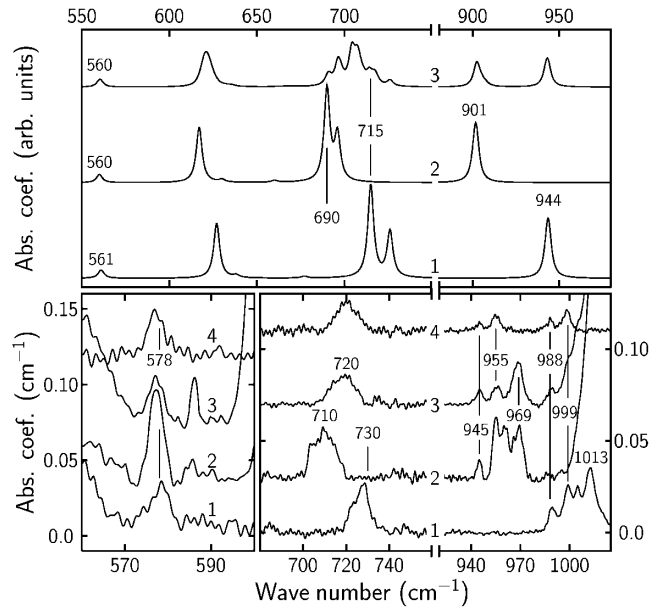


FIG. 3. Calculated (top) and observed (bottom) IR spectra for O_7 -2NN and samples described in the text. Spectra 1, 2, and 3 represent ^{16}O -rich, ^{18}O -rich, and mixed samples, respectively. In 4, the spectrum from a nonannealed mixed sample was subtracted from 3. Calculated bands are broadened with 4 cm^{-1} width Lorentzian functions. The 999 and 988 cm^{-1} bands of TDD(3) and TDD(2) shown in spectrum 1 shift to 955 and 945 cm^{-1} in spectrum 2 and remain unsplit in spectra 3 and 4. The bands at 1013 and 969 cm^{-1} in spectra 1 and 2, respectively, are those of the oxygen dimer.

at 988, 999, and 1013 cm^{-1} , respectively. The bands related to TDD are positioned in the wave number regions of 945–1000, 700–730, and 575–580 cm^{-1} . The TDD band at 580 cm^{-1} was not reported previously. A clear linear correlation was found between the integrated intensity of this band and those of the 1000 and 730 cm^{-1} bands. All of these bands possess similar formation and annealing kinetics. The 1000 and 730 cm^{-1} bands undergo upward sequential shifts (with N) of about 10 and 4 cm^{-1} , respectively, and display an oxygen origin as they shift with ^{18}O . The 580 cm^{-1} band does not shift noticeably with N or oxygen isotopic mass. By using mixtures of ^{16}O and ^{18}O , it is found that the upper band does not yield any new modes (spectra 3 and 4), suggesting that any oxygen atom is decoupled from any other oxygen atom. However, the 730 cm^{-1} band exhibits mixed modes, proving for the first time that oxygen atoms are coupled together and are in close spatial proximity.

The vibrational modes of the donors were calculated in 112 atom supercells using methods described previously [13]. To ascertain the most intense modes, we evaluated the change in their electric dipole moments by placing a charge Q on each O atom, and a charge $-mQ/2$ on each Si neighbor bonded to m O atoms. Tests with other reasonable charge distributions did not lead to significant differences.

TABLE II. Observed and calculated high frequency ^{16}O modes (cm^{-1}) of TDD(N) and O_{N+4} -2NN, respectively.

| N | 1 | 2 | 3 | 4 |
|-------|-----|-----|-----|------|
| Calc. | 940 | 951 | 963 | 969 |
| Obs. | 975 | 988 | 999 | 1006 |

The 730 and 580 cm^{-1} TDD bands can be understood as arising, respectively, from the oxygen atoms and the compressed Si bonds in the O-2NN core, while the end O-1NN atoms lead to the 1000 cm^{-1} band. The infinite O-2NN chain has only two transverse long wavelength optic modes at 814 and 564 cm^{-1} . The simple structure of the chain explains why only a few oxygen modes can be detected in each donor since only these modes can be IR active.

We now consider the oxygen-related modes arising from the ends of the chain. The highest frequency mode, evaluated directly from the dynamical matrix of all O and neighboring Si atoms in O_7 -2NN, lies at 944 cm^{-1} and is localized on the end O atoms. This frequency increases slightly to 963 cm^{-1} if only the dynamical matrices of the end Si-O-Si units are used. The modes for several donors found in this way are given in Table II. There is a 11:12:6 cm^{-1} increase with N in excellent agreement with the observed increases of 13:11:7 cm^{-1} for TDD(1), TDD(2), TDD(3), and TDD(4). Thus the model accounts for the systematic shift in the 1000 cm^{-1} band with N .

We now consider a 50-50 mixture of ^{16}O and ^{18}O atoms in O_7 -2NN and plot in Fig. 3 (top) the relative intensities of the 2^7 isotopic combinations of modes. We note that, because of its strong localization, the end mode at 944 cm^{-1} does not split, in agreement with the data. In contrast, the mode at about 715 cm^{-1} due to the O-2NN core splits in the mixed case, again in agreement with the data. Consistent with experiment, the chain model predicts that only a few absorption peaks are expected to be detected.

In conclusion, we have shown that oxygen atoms in thermal donors lie in chains along [110] with the donor activity arising from topological defects at the interfaces between two oxygen configurations. The energy levels of the topological defects lie above a Si-related [001] stress-induced gap state, and electron transfer to the latter results in a loss of oxygen parentage in the wave function. The occupation of this state is consistent with magnetic resonance and stress studies of the electronic IR transitions [17]. The model also gives stress-energy tensors, in quantitative agreement with observation, as well as points to the decrease in strain with N as the cause for the increasingly

shallow donor level. Finally, the observation and analysis of the local vibrational modes of the donors gives strong support to the model.

We acknowledge support from EPSRC and INTAS under Grant No. 97-0824. We also thank TFR, KVA, and SI in Sweden for financial support.

-
- [1] C. S. Fuller, J. A. Ditzenberger, N. B. Hannay, and E. Buchler, *Phys. Rev.* **96**, 833 (1954).
 - [2] *Early Stages of Oxygen Precipitation in Silicon*, edited by R. Jones, NATO ASI Series, Vol. 17 (Kluwer Academic, Dordrecht, 1996).
 - [3] L. C. Snyder and J. W. Corbett, in *Oxygen, Carbon, Hydrogen and Nitrogen in Silicon*, Vol. 59, p. 207, edited by J. C. Mikkelsen, S. J. Pearton, J. W. Corbett, and S. J. Pennycook, MRS Symposia Proceedings (MRS, Pittsburgh, 1985); R. Jones, *Semicond. Sci. Technol.* **5**, 255 (1990); D. J. Chadi, *Phys. Rev. Lett.* **77**, 861 (1996); M. Pesola, Young Joo Lee, J. von Boehm, M. Kaukonen, and R. M. Nieminen, *Phys. Rev. Lett.* **84**, 5343 (2000); M. Ramamoorthy and S. T. Pantelides, *Appl. Phys. Lett.* **75**, 115 (1999).
 - [4] R. C. Newman, *J. Phys. C* **18**, L967 (1985).
 - [5] P. Deák, L. C. Snyder, and J. W. Corbett, *Phys. Rev. B* **45**, 11 612 (1992).
 - [6] R. C. Newman, *J. Phys. Condens. Matter.* **12**, R335 (2000).
 - [7] L. I. Murin and V. P. Markevich, in Ref. [2], p. 329.
 - [8] D. Åberg, B. G. Svensson, T. Hallberg, and J. L. Lindström, *Phys. Rev. B* **58**, 12 944 (1998).
 - [9] J. Michel, J. R. Nicklas, and J.-M. Spaeth, *Phys. Rev. B* **40**, 1732 (1989); J.-M. Spaeth, in Ref. [2], p. 83.
 - [10] R. van Kemp, M. Sprenger, E. G. Sieverts, and C. A. J. Ammerlaan, *Phys. Rev. B* **40**, 4054 (1989).
 - [11] J. L. Lindström and T. Hallberg, *Phys. Rev. Lett.* **72**, 2729 (1994); J. L. Lindström and T. Hallberg, in Ref. [2], p. 41.
 - [12] A preliminary report will appear in *Proceedings of the ICDS'21, Giessen, 2001* (to be published).
 - [13] J. Coutinho, R. Jones, P. R. Briddon, and S. Öberg, *Phys. Rev. B* **62**, 10 824 (2000).
 - [14] Young Joo Lee, J. von Boehm, M. Pesola, and R. M. Nieminen, *Phys. Rev. Lett.* **86**, 3060 (2001).
 - [15] N. M. Johnson and S. K. Hahn, *Appl. Phys. Lett.* **48**, 709 (1986); J. Weber and D. I. Bohne, in Ref. [2], p. 123.
 - [16] D. K. Schroder, C. S. Chen, J. S. Kang, and X. D. Song, *J. Appl. Phys.* **63**, 136 (1988).
 - [17] M. Stavola, K. M. Lee, J. C. Nabity, P. E. Freeland, and L. C. Kimerling, *Phys. Rev. Lett.* **54**, 2639 (1985).
 - [18] J. M. Trombetta, G. D. Watkins, J. Hage, and P. Wagner, *J. Appl. Phys.* **81**, 1109 (1997); G. D. Watkins, in Ref. [2], p. 1.